Analytic Approximations for Moist Convectively Adjusted Regions

JIA-YUH YU* AND J. DAVID NEELIN

Department of Atmospheric Sciences, University of California, Los Angeles, Los Angeles, California

(Manuscript received 19 February 1996, in final form 30 September 1996)

ABSTRACT

Solutions are obtained for convective regions in a continuously stratified, linearized primitive equation model using a smoothly posed moist convective adjustment parameterization of cumulus convection. In the approximation in which the convective adjustment time is fast compared to other processes, the vertical structure of the temperature field is constrained to be close to the quasi-equilibrium structure determined by the convective scheme. This in turn constrains the vertical structure of the baroclinic pressure gradients and velocity field. Analytic solutions result for vertical structures, while the horizontal and time dependence is governed by equations akin to shallow water equations. These consist of equations linking baroclinic velocities and pressure gradients, plus a moist static energy equation governing thermodynamics. This system holds for basic states that are slowly varying in space, for regions where deep convection happens frequently enough to constrain the temperature field.

An effective static stability for these convectively constrained motions, the gross moist stability M, is defined in terms of thermodynamic variables. In time-dependent solutions, M determines phase speeds in deep convective regions. In solutions forced by sea surface temperature, M determines the work that must be done by vertical motion, which must in turn be balanced by surface fluxes. Surface fluxes tend to draw boundary layer temperature and moisture toward values determined by SST, while the convection translates these into deep baroclinic temperature and pressure gradients. The balance between surface fluxes and the effect of the gross moist stability on vertical motion determines how closely boundary layer enthalpy can follow SST. This picture combines modified versions of mechanisms proposed in simple models by Lindzen and Nigam, and Neelin and Held within a thermodynamically consistent framework. It also helps interpret models with convergence feedback schemes and the Gill model, and allows free parameters in these models to be related to basic thermodynamic quantities.

1. Introduction

Solutions for tropical flow in convective regions appear complex because of intricate processes involving moist convective parameterization. The eigenvalue studies of Neelin and Yu (1994, NY hereafter) and Yu and Neelin (1994, YN hereafter), however, found surprisingly simple analytic solutions using a smooth moist convective adjustment (MCA) convective parameterization. MCA is the simplest of the quasi-equilibrium (QE) class of convective parameterization, which assumes that the bulk effect of convective motions on fast timescales is to constrain the vertical profiles of buoyancy related variables. In the NY–YN study, the strong QE constraints acting on the temperature profile largely determine the vertical structure of the flow field, and it is this that facilitates analytical solutions. A notable feature of the NY–YN eigensolutions was the lack of conditional instability of the second kind, CISK, despite the crucial role of convection, so NY introduced convective interaction with dynamics (CID) as a generic acronym to refer to large-scale tropical phenomena involving interactions between large-scale dynamics and the collective effects of cumulus convection. In this paper, we follow NY's machinery and show how three-dimensional near-analytic solutions can be derived in deep convective regions when a smoothly posed MCA scheme (e.g., Betts 1986; Betts and Miller 1986) is used in a linearized primitive equation model.

As in many GCMs and simple models, the model atmosphere in this paper is set in motion by differential surface flux input, including evaporation and sensible heat, resulting from sea surface temperature (SST) anomalies. Most simple models employed in studying the atmospheric response to SST anomalies greatly simplify the complicated physical processes involving cumulus convection effects and boundary layer fluxes. The atmospheric heating anomaly is either empirically linked to the SST (Gill 1980; Gill and Rasmusson 1983) or indirectly linked to the SST through simple parameterizations of heating, surface fluxes and other feed-

* Current affiliation: Department of Atmospheric Sciences, Chinese Culture University, Yang Ming Shan, Taipei, Taiwan.

Corresponding author address: J. David Neelin, Dept. of Atmospheric Sciences, University of California, Los Angeles, Los Angeles, CA 90024-1565.
E-mail: neelin@nino.atmos.ucla.edu

back mechanisms (Webster 1981; Zebiak 1982, 1986; Weare 1986; Kleeman 1991). Neelin and Held (1987) approached the atmosphere coupling to SST in the Tropics by using the moist static energy budget. They claimed that the time-mean low-level convergence in the tropical atmosphere is associated with the small value of the effective moist stability. A seemingly different approach was proposed by Lindzen and Nigam (1987). They assumed that the SST gradient can affect the boundary layer temperature gradient through turbulent vertical mixing, which in turn yields a pressure gradient force to drive the boundary layer flow.

In spite of the fact that simple models have bypassed complicated physical processes, these models can sometimes behave qualitatively similar to GCM simulations and even to the observations. This suggests that some important dynamical processes responsible for the atmospheric response may have been captured by some of these simple assumptions. However, the simple models often produce indistinguishably similar simulations based on very different physical assumptions (Neelin 1989). This disagreement suggests that we lack a firm understanding of the exact mechanisms driving even the most basic of tropical climate features, such as the Walker circulation and the ITCZ. The ambiguity arises from the fact that the convective interaction with dynamics, which is of crucial importance for tropical dynamics, is at best crudely represented. By employing a model that includes a cumulus parameterization closely related to one used in some GCMs that can better resolve the vertical structures of the dynamics, one might hope to distinguish among the hypothesized mechanisms, to explain why the simple models sometimes work, and to understand their limitations.

Section 2 displays complete formulation of the linearized primitive equation model, including cumulus convection and surface flux parameterizations. Section 3 provides the analytical approach toward the asymptotic solutions, including discussion of the QE assumptions employed by the Betts–Miller MCA scheme and the resulting dynamic system. Section 4 discusses the model behavior, including implications of the model for other simpler models, and provides an example for a simple Gill-like case. Conclusions are presented in section 5.

2. Model equations and physics

The primitive equations linearized about a continuously stratified basic state in radiative–convective equilibrium [see (2.2.a)–(2.2.c) of NY for details] can be expressed as

$$(\partial_t + \overline{\mathcal{D}}_m)\mathbf{v}' + f\mathbf{k} \times \mathbf{v}' + \nabla\phi' = 0, \qquad (2.1a)$$

$$\phi' = \phi_0' + \kappa \int_{p_0}^{p} T\, d\ln p, \qquad (2.1b)$$

$$\nabla\cdot\mathbf{v}' + \partial_p\omega' = 0, \qquad (2.1c)$$

$$(\partial_t + \overline{\mathcal{D}}_T + \epsilon_r)T' + (\partial_p\overline{s})\omega' = Q_c' + g\partial_p F_T', \qquad (2.1d)$$

$$(\partial_t + \overline{\mathcal{D}}_T)q' + (\partial_p\overline{q})\omega' = Q_q' + g\partial_p F_q', \qquad (2.1e)$$

where $\mathbf{v}'$, ϕ, ω', T', and q' denote perturbations of horizontal wind (in vector form), geopotential height, pressure velocity, temperature, and specific humidity, respectively. Notation $\mathbf{k}$ denotes the upward unit vector, $\kappa = R/C_p$ denotes the ratio of gas constant to heat capacity at constant pressure, and $\partial_p\overline{s}$ and $\partial_p\overline{q}$ denote stratifications of basic-state dry static energy and specific humidity in the troposphere. Here, Q_c' andQ_q' denote the convective heating and moisture source perturbations due to subgrid-scale cumulus convection. They are functions of perturbations and basic-state thermodynamic quantities (T', q',T_b', q_b', $\overline{T}$), as will be specified in the cumulus parameterization later. For brevity, we have absorbed C_p (L) into temperature (specific humidity) in (2.1b), (2.1d), and (2.1e) so they both have energy units (J kg^{-1}).

In (2.1a), (2.1d), and (2.1e), we have defined two linear operators,

$$\overline{\mathcal{D}}_m = \overline{\mathbf{U}}\cdot\nabla + A_m\nabla^2 + \epsilon_m, \qquad (2.2a)$$

$$\overline{\mathcal{D}}_T = \overline{\mathbf{U}}\cdot\nabla + A_h\nabla^2, \qquad (2.2b)$$

where $\overline{U}$ is the barotropic mean zonal wind, A_m and A_h denote the horizontal diffusion coefficients for the momentum and temperature (moisture) equations, and ϵ_m represents the Rayleigh friction damping rate. We note that $\overline{D}_m$ and $\overline{D}_T$ have to be barotropic to get the analytic approximations. Vertical diffusions of T' and q' are left implicitly in flux forms, with F_T' and F_q' (both in units of J m^{-2} s^{-1}) denoting the sensible heat flux and moisture flux, respectively. For the boundary conditions, we let both fluxes vanish at the model top but approach, respectively, surface sensible heat flux and surface evaporation at the surface (i.e., $F_T' = H'$ and $F_q' = E'$ at $p = p_0$). Also in (2.1a) and (2.1d), we have used a simple Rayleigh damping and a simple Newtonian cooling term in momentum and temperature equations to crudely represent the radiative and frictional damping effects in the model.

a. Parameterization of cumulus convection

The collective effects of cumulus convection are parameterized using the Betts–Miller (Betts 1986; Betts and Miller 1986) MCA scheme. The Betts–Miller scheme is a gentler version of the MCA due to the introduction of a relaxation time, τ_c, in smoothly adjusting temperature and moisture toward selected reference profiles. The convective heating and moisture source are represented as

$$Q_c' = \tau_c^{-1}(T_c' - T' - \Delta T_c'), \qquad (2.3a)$$

$$Q_q' = \tau_c^{-1}(q_c' - q'), \qquad (2.3b)$$

where T_c' and q_c' are the temperature and specific humidity reference profiles toward which convective adjustment occurs, which are themselves functions of the basic-state and large-scale thermodynamic variables. Here, $\Delta T_c'$ is a temperature correction to satisfy the moist enthalpy conservation constraint in the column from cloud top (p_T) down to sea surface level (p_0):

$$\int_{p_\mathrm{T}}^{p_0} Q_c' \frac{dp}{g} + \int_{p_\mathrm{T}}^{p_0} Q_q' \frac{dp}{g} = 0, \tag{2.4}$$

which is nonlocal in the vertical. In the analytical approach, this yields a correction term for the moist enthalpy conservation constraint. Assuming the temperature correction is constant in the vertical,

$$\Delta T_c' = \Delta p_\mathrm{T}^{-1} \left[\int_{p_\mathrm{T}}^{p_0} (T_c' - T')\, dp + \int_{p_\mathrm{T}}^{p_0} (q_c' - q')\, dp \right], \tag{2.5}$$

where Δp_T is defined as the total length column over which the moist processes take place. We note that the part of heating associated with adjustment toward reference profiles [i.e., $\tau_c^{-1}(T_c' - T')$] stops at the cloud base, while the energy correction term ($\Delta T_c'$) is applied in the heating column, including cloud base.

Following NY–YN, the temperature reference profile can be expressed in terms of a simple function of the boundary layer thermodynamic quantity h_b':

$$T_c' = A(p,x,y)h_\mathrm{b}', \tag{2.6}$$

where $h_\mathrm{b}' = (T_\mathrm{b}' + q_\mathrm{b}')$ is the boundary layer moist enthalpy, and T_b' and q_b' denote the temperature and specific humidity perturbations at the bottom of the planetary boundary layer (PBL). Here, $A(p,x,y)$ denotes the three-dimensional dependence of the temperature reference profile on h_b'. Its structure is a function of the basic-state thermodynamic variables. Using a dry adiabat within the PBL and moist adiabat from the top of the PBL yields

$$A(p, x, y) = (1 + \gamma)^{-1}(p_\mathrm{b}/p_0)^\kappa \times \exp\left[-\kappa \int_p^{p_\mathrm{b}} (1 + \gamma)^{-1}\, d\ln p \right], \quad p_\mathrm{b} \geq p \geq p_\mathrm{T}; \tag{2.7a}$$

$$A(p, x, y) = (1 + \gamma_b)^{-1}(p/p_0), \quad p_0 \geq p \geq p_\mathrm{b}; \tag{2.7b}$$

where $\gamma = (dq_\mathrm{sat}/dT)|_{\overline{T}}$ and q_sat is the saturation specific humidity. This is appropriate to a parcel rising from the bottom of the PBL or from anywhere within a well-mixed PBL, taking saturation to occur at p_b'.

Also following NY–YN, the moisture reference profile is chosen to have a given fraction of saturation; that is,

$$q_c' = \alpha q_\mathrm{sat}' = \alpha\gamma T'. \tag{2.8}$$

Here, $\alpha = 1$ denotes 100% saturation. In the numerical calculations in section 4c, we let the moisture profile be subsaturated ($\alpha < 1$) in the convective column, as may be observed in most precipitating regions.

b. Parameterization of surface fluxes

To incorporate the boundary layer fluxes into the model, two bulk formulas are used for the linearized surface sensible heat flux (H') and surface evaporation (E'). Following NY, they are given by

$$(g/\Delta p_\mathrm{T})H' = \epsilon_T[T_s' - (p_0/p_\mathrm{b})^\kappa T_b'] - Fu_0', \tag{2.9a}$$

$$(g/\Delta p_\mathrm{T})E' = \epsilon_T[\gamma_0 T_s' - q_b'] - Gu_0', \tag{2.9b}$$

where $\boldsymbol{\epsilon}_T = \rho C_D \overline{W}(\Delta p_\mathrm{T}/g)^{-1}$ is a damping rate associated with temperature and moisture per unit tropospheric depth (Δp_T); $\overline{W}$ denotes the mean surface wind speed, which is potentially a function of space; ρ is the density of air; C_D is the surface exchange coefficient (or drag coefficient); $\gamma_0 = (dq_\mathrm{sat}/dT)|_{\overline{T}_0}$; and T_s' denotes the SST perturbation. Estimates of $\boldsymbol{\epsilon}_T$ suggest a magnitude on the order of (10 days)$^{-1}$ to (20 days)$^{-1}$, depending on the values of parameters. The second terms on the rhs of (2.9a) and (2.9b) represent the wind feedback mechanisms with evaporation–wind feedback constant F and sensible heat flux wind feedback constant G:

$$F = -(dW/du_0)(g/\Delta p_\mathrm{T})\rho C_D(\overline{q}_\mathrm{sat}(T_s) - \overline{q}_b), \tag{2.10a}$$

$$G = -(dW/du_0)(g/\Delta p_\mathrm{T})\rho C_D(\overline{T}_s - \overline{T}_\mathrm{b}), \tag{2.10b}$$

where u_0 is the surface zonal wind and u_0' in (2.9a) and (2.b) is its perturbation part.

The SST forcing enters the boundary layer thermodynamics through both the surface sensible heat flux and the surface evaporation in (2.9a) and (2.9b). The subsequent release of latent heat in the cumulus convection then redistributes the moist enthalpy in vertical to maintain a thermodynamically consistent three-dimensional circulation. We also note that only surface flux terms associated with T_s' contribute to the forcing by SST. The other part of the fluxes (notably terms associated with T_b' and q_b') belongs to a portion of the response, so fluxes are determined as part of the response to the SST forcing. The forcing term $\epsilon_T(1 + \gamma_0)T_s'$ is much larger than the fluxes themselves, since there is cancellation within the fluxes.

3. Analytical framework

In a time-dependent case, linearized about a homogeneous basic state, NY–YN found that the convective QE constraints select a unique vertical mode, the propagating deep convective mode characterized by the slow timescale and near-adjusted thermodynamic structures, as the only geophysically interesting mode arising through CID at large scales. Motivated by those results, we anticipate that the QE constraints will yield similar simplifications for the tropical large-scale, slowly varying flow forced by SST distribution in the lower boundary. Here, we mimic NY's machinery and show how three-dimensional near-analytic flow can be derived through MCA's convective constraints in deep convective regions.

a. Convective quasi-equilibrium constraints

In this paper, analytic approximations of the model come from a perturbation expansion based on the convective QE assumptions. More precisely, we assume that the timescale τ_c at which sub-Reynolds-scale convective processes remove convective available potential energy is much shorter than either the timescale of large-scale variability or any of the timescale parameters characterizing the dynamics of the time-mean circulation (e.g., timescales associated with damping, effects of stratification on large-scale motions, etc.).

Expanding all perturbation variables in orders of τ_c, $(\ ) = (\ )^{(0)} + \tau_c(\ )^{(1)} + \tau_c^2(\ )^{(2)} + \cdots$, and using the MCA temperature closure (2.6) on the T reference profile, the order unity [i.e., $O(\tau_c^0)$] balance yields

$$T^{(0)} = A(p, x, y)h_{\mathrm{b}}^{(0)}. \tag{3.1}$$

If we further use the MCA moisture closure (2.8), we can get

$$q^{(0)} = \alpha\gamma A(p, x, y)h_{\mathrm{b}}^{(0)} \tag{3.2}$$

and a simple relation between h_{b} and T_{b}:

$$h_{\mathrm{b}}^{(0)} = (1 + \alpha_{\mathrm{b}}\gamma_{\mathrm{b}})T_{\mathrm{b}}^{(0)}. \tag{3.3}$$

Since only the zeroth-order (QE) thermodynamic variables are needed for a closed set of equations, we neglect all superscripts hereafter for brevity.

b. Asymptotic solutions for slowly varying basic states

To simplify the problem for near-analytic solutions, we assume that the basic state is only slowly varying in the Tropics. That is, we assume that the length scale associated with horizontal variations of the basic state (L) is large compared to the length scales associated with perturbations of interest (l). This condition can always be obtained in principle by making the SST distribution that forces the basic state flatter and flatter so that the homogeneous case is approached. Some basic-state quantities thus may be expressed as

$$\begin{aligned}&\bar{s} = \bar{s}(p, \eta x, \eta y), \bar{q} = \bar{q}\,(p, \eta x, \eta y),\\ &A = A(p, \eta x, \eta y),\end{aligned} \tag{3.4}$$

where $\eta = l/L$ is a small (or slow) parameter. We note that, under these assumptions, the gradients of the above basic-state quantities are on the order of η.

With the QE constraint (3.1) in the momentum and hydrostatic equations (2.1a) and (2.1b) (and taking the momentum damping rate ϵ_m constant in p), the solutions for horizontal velocity can be written as

$$\mathbf{v}(x, y, p, t) = \mathbf{v}_T(x, y, t)A^+(p, \eta x, \eta y) + \mathbf{v}_0(x, y, t), \tag{3.5}$$

where $\mathbf{v}_\mathbf{T}$ provides the spatial and time dependence of the part of circulation associated with the QE-driven baroclinic component, and $\mathbf{v}_0$ is the surface wind. Integrating the continuity equation (2.1c) from any level p in the troposphere down to the surface level p_0 and using (3.5) yields

$$\omega = \omega_0 + \int_p^{p_0} (A^+\nabla\cdot\mathbf{v}_T + \nabla\cdot\mathbf{v}_0)\, dp', \tag{3.6}$$

where ω_0 is the pressure velocity at surface level due to the existence of topography and

$$A^+(p, \eta x, \eta y) = \kappa \int_p^{p_0} A(p', \eta x, \eta y)\, d\ln p'. \tag{3.7}$$

If we use the rigid-lid condition and neglect topography (i.e., $\omega_T = 0$ and $\omega_0 = 0$), we get a simple relation between $\mathbf{v}_T$ and $\mathbf{v}_0$:

$$\mathbf{v}_0 = -\widehat{A^+}\mathbf{v}_T + O(\eta), \tag{3.8}$$

where $\widehat{A^+} = \Delta p_T^{-1}\int_{p_T}^{p_0} A^+dp$ denotes the vertically averaged quantity. Thus ω becomes

$$\omega = \left[\int_p^{p_0} (A^+ - \widehat{A^+})\, dp\right] \nabla\cdot\mathbf{v}_T + O(\eta). \tag{3.9}$$

For the kinematic part, using (2.1b) in (2.1a) and then subtracting the latter from its surface level part, the flow implied by the QE thermodynamic constraints becomes

$$(\partial_t + \overline{\mathcal{D}}_m)\mathbf{v}_T + \beta y\mathbf{k} \times \mathbf{v}_T + \nabla h_{\mathrm{b}} = 0, \tag{3.10}$$

where we have neglected terms of $O(\eta)$ or smaller in (3.10). As noted from (3.10), the QE constraints acting on $\nabla\phi$ through the T reference profile greatly simplify the kinematics of the tropical circulation.

For the thermodynamic part, since heating and moisture sink are not quantities that need to be treated directly in the analytical approach under the QE constraints (they are obtained diagnostically from the solutions), we can use the vertically integrated moist static energy equation implied by (2.4) to replace the thermodynamic equations. Neglecting both wind feedback terms in (2.9a) and (2.9b), the order τ_c energy constraint becomes simply the vertically integrated moist static energy equation

$$\begin{aligned}&[(\partial_t + \mathcal{D}_T)A^* + (\hat{A}\epsilon_r + \epsilon_T)]h_b\\ &\quad + \Delta p_T^{-1}\int_{p_{\mathrm{T}}}^{p_0} (\partial_p\bar{h})\omega\, dp = (1 + \gamma_0)\epsilon_T T_s,\end{aligned} \tag{3.11}$$

where

$$A^*(\eta x, \eta y) = \hat{A} + \widehat{\alpha\gamma A}. \tag{3.12}$$

A suitable upper-boundary condition is required for

(3.11) to get the three-dimensional tropical circulation forced by SST anomalies. For the simplest rigid-lid case, under the slowly varying basic-state assumptions considered here, the cloud top (p_{T}) is also a slowly varying function of x and y. Thus the cloud-top pressure velocity (ω_{T}) is on the order of η. This is a handy property since the order unity balances are automatically closed to form a neat analytical expression of the atmospheric response to SST anomalies while, at the same time, permitting the horizontal inhomogeneity of the thermodynamic basic states to order η. The radiation condition does not qualitatively change the dynamics of the large-scale tropospheric motions constrained by convection of concern here. It only gives a small correction to the propagation tendency and introduces scale selectivity favoring planetary scale waves, as pointed out by NY and Yano and Emanuel (1991).

Using (3.9) in (3.11) and neglecting terms of $O(\eta)$ gives the following QE moist static energy equation:

$$[(\partial_t + \overline{\mathcal{D}}_T)A^* + (\hat{A}\epsilon_r + \epsilon_T)]h_{\mathrm{b}} + M\nabla\cdot\mathbf{v}_T = (1 + \gamma_0)\epsilon_T T_s, \tag{3.13}$$

where M (in units of J kg^{-1}) is defined as

$$M(\eta x, \eta y) = \Delta p_T^{-1}\int_{p_{\mathrm{T}}}^{p_0}(\partial_p\overline{h})\int_p^{p_0}(A^+ - \widehat{A^+})\,dp'\,dp. \tag{3.14}$$

The "gross moist stability" M represents the net static stability in the troposphere, including moisture effects, felt by the QE perturbations. It was first defined by Neelin and Held (1987) in a two-level model and was later redefined more precisely by NY in a homogeneous basic state. We note that, except for using p_0 as the reference level and permitting a slowly varying basic state, the expression (3.14) is identical to that of NY. The derivation above not only gives a precise meaning to the gross moist stability, but also to the net thermodynamic damping in a vertically continuous atmosphere. An estimate of M using Jordan's (1958) sounding profile suggests a value of about 180 J kg^{-1} (NY), corresponding to the phase speed of about 13 m s^{-1}. This value is much smaller than the phase speed for dry wave motions. Detailed discussion of (3.14) and its implications to other simple models is presented in section 4.

The wind feedback mechanisms of (2.9a) and (2.9b) have been omitted for clarity in (3.13). These simply add a term F^*u_T' with $F^* = -(F + G)\widehat{A^+}u_T$, and F and G as in (2.10a) and (2.10b). Equations (3.10) and (3.13), along with the two diagnostic equations (3.8) and (3.9), form a closed set of equations for the three-dimensional tropical flow forced by SST. The economy of this model comes from the fact that the QE assumptions determine the vertical structure of the dynamic response. Once the associated horizontal response is solved for, the three-dimensional structures of the tropical flow can be readily reconstructed.

4. Model behavior

The internal variability of the model presented in the previous section for the unforced case yields results similar to those of NY–YN. We omit the discussion here and focus on the steady-state behavior of the model. To facilitate discussion, we also let $\overline{\mathcal{D}}_m = \epsilon_m$ and $\overline{\mathcal{D}}_T = 0$. This makes the kinematic part of the model similar to the Gill-like models. However, the thermodynamic part of the model is still considerably improved compared to most simple models in the sense that cumulus convection and boundary layer flux parameterizations are approximations to those that are used or could be used in a GCM.

a. Gross moisture stratification

Due to the explicit representation of moisture processes in the model, the precipitation rate (P) can be directly calculated from the moisture budget:

$$P = E + \frac{\Delta p_{\mathrm{T}}}{g}M_q\nabla\cdot\mathbf{v}_T, \tag{4.1}$$

where

$$M_q(\eta x, \eta y) = -\Delta p_T^{-1}\int_{p_{\mathrm{T}}}^{p_0}(\partial_p\overline{q})\int_p^{p_0}(A^+ - \widehat{A^+})\,dp'\,dp \tag{4.2}$$

is termed the "gross moisture stratification," denoting the part of M due to stratification of moisture. Roughly speaking, M_q measures the moisture available for precipitation from moisture convergence in deep convective regions. As noted in (4.1), the precipitation pattern is in phase with the large-scale convergence. However, the precipitation strength is dictated by both M_q and $\mathbf{v}_T$.

To obtain a feeling for how the precipitation depends on the dynamics consider the case where the M term would dominate the balance on the lhs of the QE moist state energy equation (3.13) (the physical situations where this would hold depend as much on the scales of forcing as on the magnitude of M and the thermodynamic damping terms). Then the moisture convergence contribution to the precipitation pattern is directly proportional to the SST forcing, with the amplitude determined by the ratio of gross moist stratification to gross moist stability; that is,

$$P \propto (M_q M^{-1})T_s. \tag{4.3}$$

In the opposite case, where the thermodynamic damping terms dominate in (3.13), h_{b} rather than the convergence is proportional to T_s. For the precipitation pattern, this implies smaller scales due to wave dynamics, and it tends to concentrate near the SST anomaly maximum.

b. Comparison with simpler models

Using (3.10) to eliminate $\mathbf{v}_T$ through the relation $\nabla\cdot\mathbf{v}_T = \mathcal{L}_{x,y}h_b$, we can rewrite the moist static energy equation (3.13) as

$$[(\hat{A}\epsilon_r + \epsilon_T) - M\mathcal{L}_{x,y}]h_b = (1 + \gamma_0)\epsilon_T T_s, \quad (4.4)$$

where

$$\mathcal{L}_{x,y} = \frac{\epsilon_m}{(\epsilon_m^2 + f^2)}\partial_x^2 + \frac{\beta(f^2 - \epsilon_m^2)}{(\epsilon_m^2 + f^2)^2}\partial_x + \frac{\epsilon_m}{(\epsilon_m^2 + f^2)}\partial_y^2 - \frac{2\epsilon_m\beta f}{(\epsilon_m^2 + f^2)^2}\partial_y \quad (4.5)$$

is a linear operator in space. Physically, inversion of this operator implies redistribution of the atmospheric response to SST forcing by wave dynamics. In (4.5), $\beta = df/dy$ and the second derivative of f has been neglected. We note that, as f becomes large, the $\mathcal{L}_{x,y}$ term in (4.4) becomes less important. The atmosphere thus exhibits less nonlocal response in h_b and $\mathbf{v_T}$ away from the equator. Near the equator, M gives nonlocal response in steady-state cases and its value is of crucial importance to winds in the equatorial waveguide.

The analytic approximations for the simplest case (i.e., using Raleigh friction in the momentum equation and Newtonian cooling in the temperature equation) presented here provide links to many of the simpler atmospheric models that currently reign in the coupled model studies (e.g., Gill 1980; Lindzen and Nigam 1987; Zebiak 1982, 1986; etc.). In particular, it yields the QE moist static energy equation (4.4) with an internally defined stability parameter, M, appearing in a term associated with the large-scale convergence. We note that, even though (4.4) is expressed in terms of the boundary layer moist enthalpy h_b, the boundary layer dynamics is not isolated from the troposphere but feels the moist stratification of the troposphere through M. This differs from many simpler models in which the boundary layer dynamics is isolated from the atmosphere above.

The simplifications of tropical dynamics implied by the QE assumptions may also help justify important aspects of some simple models. In particular, there are some strong parallels between our model and the Lindzen and Nigam (1987) model. The Lindzen–Nigam model was primarily concerned with examining the consequences of pressure gradients produced within the trade wind boundary layer by the SST gradients below. The role of deep convection was conceived as responding with a cumulus mass flux that carries converged mass from the boundary layer to sufficient heights that the pressure gradients associated with its divergence can be neglected. Despite these differences in approach, the fundamental connection between the models is that *strong thermodynamic constraints determine the dynamics through horizontal pressure (geopotential) gradients implied by the hydrostatic balance.* In our model, the thermodynamic constraints are applied through moist adjustment by deep convection, rather than through vertical mixing, and the entire column enters the picture rather than just the layer below the trade inversion, but the principle is the same.

There are equally strong parallels to the model of Neelin and Held (1987). The term $M\mathcal{L}_{x,y}h_b$ in (4.4) is proportional to the gross moist stability times the vertical velocity at the top of boundary layer, and the precipitation typically follows the pattern of SST forcing, with its amplitude modulated by moist stratification. The main difference between the Lindzen–Nigam and Neelin–Held models lies in the fact that the boundary layer temperature does not exactly follow the SST but rather is "spread out" by the dynamics due to inversion of $\mathcal{L}_{x,y}$. The amplitude of h_b depends on a balance of moist stratification and thermal damping processes due to surface fluxes and radiative effects. The latter implies that boundary layer temperature is never brought exactly to T_s no matter how small M is. Thus, at least in the context of a MCA scheme, the model presented here reconciles Lindzen–Nigam and Neelin–Held approaches. If reconsidered in terms of the present model (for small anomalies on a slowly varying basic state dominated by deep convection), there is no fundamental contradiction between approaches based on (i) constraints on baroclinic pressure gradients (akin to Lindzen–Nigam) or (ii) moist static energy conservation and an effective static stability for large-scale convective motions (akin to Neelin–Held).

We also note that the analytic approximations in (3.10) and (3.13) are similar in form to the Gill-like models (Gill 1980; Zebiak 1982, 1986; Lindzen and Nigam 1987; Neelin 1989) if the following parameter equivalence is made:

$$c^2 \equiv M/A^*, \qquad \epsilon_T \equiv (\hat{A}\epsilon_r + \epsilon_T)/A^*, \quad \text{and}$$
$$Q \equiv (1 + \gamma_0)(\epsilon_T/A^*)T_s, \quad (4.6)$$

where c is the phase speed for a prescribed internal mode, ϵ_T is the thermal damping rate in height equation, and Q is the prescribed heating in the Gill-like models. Even though the simplest form of our solution is similar to the Gill-like models, it has several advantages in terms of interpretation. In particular, the propagation characteristics are internally determined by the gross moist stability (M), which is explicitly defined in terms of basic-state thermodynamic parameters and which permits horizontal inhomogeneity instead of being an arbitrarily specified constant in the Gill-like models. The thermal damping is also defined more precisely and includes radiative cooling and damping effects due to the parts of sensible heat and evaporation related to the boundary layer temperature and moisture perturbations. The forcing sources come from the parts of the sensible heat and evaporation fluxes related to T_s and $q_{\text{sat}}(T_s)$ (forcing due to the latter is usually much larger than the former). Thus both sensible heat and evaporation fluxes

TABLE 1. Magnitude of some constants used to construct the atmospheric response to SST forcing in the Gill-like version of the model. Here, M and M_q are calculated from Jordan's (1958) sounding profile.

Parameter	Symbol	Value
Gross moist stability	M	180 J kg^{-1}
Gross moisture stratification	M_q	1000 J kg^{-1}
Cloud-top pressure	p_T	150 mb
Cloud-base pressure	p_b	950 mb
Sea surface level	p_0	1000 mb
Tropospheric depth	Δp_T	850 mb
Mechanical damping rate	ϵ_m	(2 days)$^{-1}$
Newtonian cooling rate	ϵ_r	(10 days)$^{-1}$
Surface exchange coefficient	C_D	1.5×10^{-3}
Effective damping rate by E and SH implied by C_D	ϵ_T	(20 days)$^{-1}$

are also internally determined by the response, not just by the forcing alone.

c. A Gill-like case

To understand the most basic dynamics of the model and show the relationship between familiar two-dimensional Gill-model solutions and three-dimensional flows dominated by deep convection, an idealized positive SST anomaly pattern is used to force the simplest form of the model. This idealized positive SST pattern (not shown) has a half sinusoidal distribution in longitude from 160°E to 120°W with a maximum of 1 K at 160°W, 6°S. Its magnitude decays quickly in meridional direction as a Gaussian with a *e*-folding scale of 6° latitude. We note that spatial distributions of M and M_q can be directly estimated from sounding data (Yu et al. 1997). For the moment, we let M be constant in the whole domain of interest in order to compare the model with the Gill (1980) solutions. Values of M, M_q, and other thermodynamic variables presented in section 3 are calculated using Jordan's (1958) sounding profile. Table 1 summarizes important parameters used in this section.

Since the kinematic part of this model is similar to the Gill model (1980) and its solutions are familiar to many readers, we focus on the three-dimensional thermodynamic response. Figure 1 shows the model temperature at the bottom of the PBL (T_b) and precipitation (P) in response to the SST forcing. As expected from (4.4), T_b does not exactly follow the SST distribution but is modified by the moist wave dynamics. In particular, T_b is more locally confined near the SST anomaly center in the Southern Hemisphere than in the Northern Hemisphere. We also note that the amplitude of T_b is far less than the associated SST anomalies. This behavior was noted also by Raymond (1994) in a simple tropical circulation model. The maximum value of T_b is just slightly over 0.2 K, compared to the maximum SST anomaly of 1 K. The precipitation perturbations (i.e., convergence zone), however, show strong resemblance to the SST pattern. The positive precipitation perturbations roughly follow the SST pattern with a maximum value over 4 mm day^{-1}. We note that there is a slight tendency of southeast extension in the convergence zone even though the SST does not provide this tendency. The negative precipitation perturbations are found to the north and to the east of the positive SST anomalies, associated with local asymmetric Hadley and Walker circulations in these regions. As discussed following (4.5), for a larger-scale SST anomaly, T_b would follow SST more closely and precipitation would follow it less closely.

Figures 2a–c display the latitude–height sections of the atmospheric response in temperature, pressure velocity, and specific humidity, respectively, along 160°W longitude. In Fig. 2a, the temperature perturbation has larger amplitude in the upper troposphere with a maximum value just over 0.5 K and with the vertical structure dictated by the strong convective constraints under MCA's QE assumptions. Vertical motion (Fig. 2b) has maximum amplitude at about 450 mb and a single sign throughout the troposphere, again related to QE con-

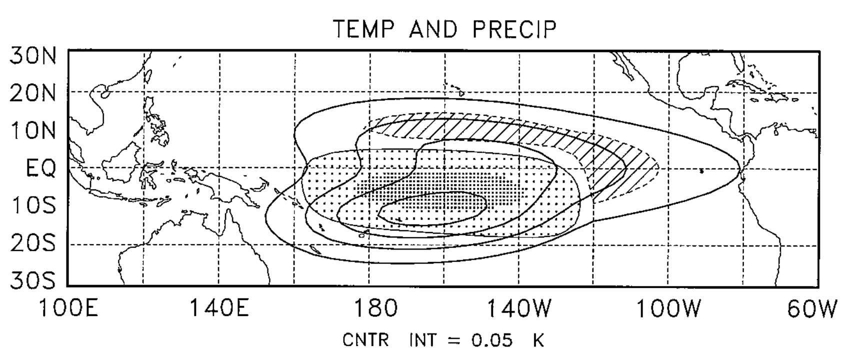

FIG. 1. Boundary layer temperature (contours) and precipitation (shading) perturbations in the Gill-like case for a simple SST forcing. Contour interval is 0.05 K. Hatched area denotes negative precipitation perturbations, and dotted area denotes positive precipitation perturbations. Positive precipitation larger than 2 mm day^{-1} is shown by dense dots. Continental outlines are for scale reference only. The SST forcing pattern (described in the text) is very similar to the region of positive precipitation with a maximum of 1 K at 160°W, 6°S.

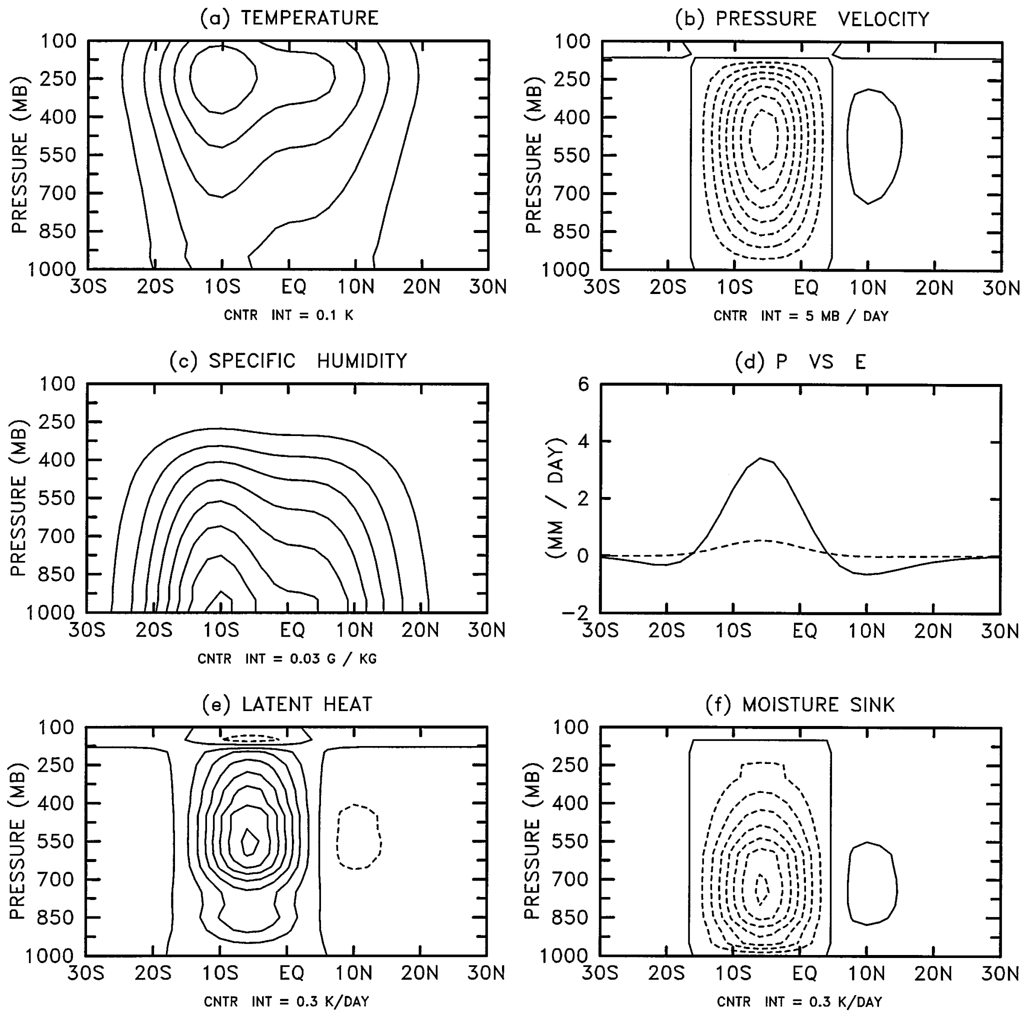

FIG. 2. Latitude–height sections of the atmospheric response along 160°W longitude in (a) pressure velocity, (b) temperature, (c) specific humidity, (d) precipitation contributions due to the moisture convergence (solid line) and local evaporation (dashed line), (e) latent heating (Q_c), and (f) moisture source ($-Q_q$). Solid lines in (a), (b), (c), (e), and (f) denote positive perturbations; dashed lines denote negative perturbations. The contour intervals in (a), (b), (c), (e), and (f) are 5 mb day^{-1}, 0.1 K, 0.03 g kg^{-1}, 0.3 K day^{-1}, and 0.3 K day^{-1}, respectively.

straints. The horizontal distribution has upward motion roughly over regions of positive SST anomalies. The rising motion is compensated in longitude as well as latitude so the descending branch south of the SST forcing is weak. Significant moisture perturbations are confined to the lower troposphere (Fig. 2c) with a vertical profile given by the moisture closure (3.2). The maximum amplitude, determined by horizontal dynamics, reaches 0.25 g kg^{-1} in the PBL. This can be compared to the difference $q'_{\mathrm{sat}}(T_s)$ of about 1 g kg^{-1} created by the SST anomaly. As with temperature, the nonlocal dynamics prevents q'_b from approaching $q'_{\mathrm{sat}}(T_s)$ too closely, thus creating evaporation in that region.

Figure 2d compares the precipitation due purely to moisture convergence (solid line) with the local evaporation (dashed line). Both curves roughly follow the SST anomaly pattern with positive response over positive SST regions. The precipitation perturbation due purely to the moisture convergence is much larger than the local evaporation over positive SST anomaly regions. This is as expected but serves to indicate the dominance of nonlocal processes by CID in determining the atmospheric response to the SST anomaly forcing. If the evaporation–wind feedback were included, the evaporation structure could change substantially but the precipitation pattern would be less altered.

Figures 2e and 2f show the convective heating (Q_c) and moisture source (Q_q) perturbations calculated diagnostically from (2.1d) and (2.1e). Since Q_c and Q_q terms are mostly balanced by the adiabatic process (i.e., $\omega\partial_p\bar{s}$ and $\omega\partial_p\bar{q}$) in the deep convective regions, we have neglected contributions from the diffusive fluxes in these figures. In Fig. 2e, consistent with the vertical velocity profile, heating (cooling) is found throughout the troposphere in the ascending (descending) regions and the maximum heating rate can reach 2 K day^{-1}, while in Fig. 2f, the moisture sink (source) is found in ascending (descending) regions. The higher maximum of heating versus moisture sink comes from the structure of $\partial_p\overline{s}$ and $\partial_p\overline{q}$ in Jordan's (1958) profile.

5. Conclusions

Simple analytic solutions are presented for deep convective regions in a linearized primitive equation model, based on the quasi-equilibrium assumptions of a moist convective adjustment convective parameterization. The QE assumptions, in which both temperature and moisture are assumed nearly in adjustment with the reference profiles, greatly simplify the dynamic response of the tropical flow through strong constraints acting on the thermodynamic profiles. The model solution separates into vertical structures determined by the thermodynamic constraints and equations in (x,y,t) for horizontal structures, akin to shallow water equations. The thermodynamics is governed by a simple form of the QE moist static energy equation (3.13). Two internally defined parameters arise: the gross moist stability (M) and the gross moisture stratification (M_q). The first acts as an effective static stability for the system, determining phase speeds and affecting response to external forcing. The latter is important to precipitation, although it does not directly impact the dynamics. Both are examined in data by J.-Y. Yu et al. (1997, manuscript submitted to *J. Atmos. Sci.*), where spatial variations of these are considered. Our derivation permits horizontal inhomogeneity of the basic state, provided it has sufficiently small spatial derivatives. This solution provides a detailed example of the implications of ''quasi-equilibrium thinking'' advocated by Emanuel et al. (1994).

The horizontal structure equations of the QE-based model can be simplified to a Gill (1980) model if the parameters of the latter are suitably redefined. However, the model has several advantages over the Gill-like models in terms of physical interpretation. In particular, the model produces a three-dimensional, thermodynamically consistent circulation. Also, instead of being arbitrarily specified as in the Gill-like models, the propagation tendency (dictated by M) can be directly estimated from the atmospheric sounding profiles. The thermal damping used in Gill-like models is also better defined in our model. It results from a combination of the longwave radiation and contributions from the sensible heat and evaporation.

The analytical solutions give some insights into simple models and into the mechanisms by which SST drives tropical circulation. The role of convective interaction with dynamics enters most strongly via the constraints convection places on the large-scale circulation by determining the vertical structure of baroclinic pressure gradients. The SST forcing enters the boundary layer thermodynamics through evaporation and sensible heat fluxes, which are calculated internally as part of the atmospheric response (as in a GCM and in contrast to some simple models). The entire tropospheric thermodynamics participates in determining the response (through M) rather than just the layer below the trade inversion as in some simple models, notably Lindzen and Nigam (1987). While surface fluxes tend to bring the PBL temperature and moisture toward values given by SST, changes in PBL moist static energy are translated by convection into baroclinic pressure gradients. Vertical motions implied by these must do work against the gross moist stability. This has the effect of making the solutions nonlocal in the horizontal and preventing PBL moisture and temperature from entirely adjusting to local SST. The solution results from the balance of surface fluxes versus moist wave dynamics governed by the gross moist stability.

This balance of mechanisms contains elements of both the Lindzen–Nigam (1987) and Neelin–Held (1987) mechanisms, permitting a reconciliation of these views. As in the Lindzen–Nigam view, strong constraints on temperature determine the dynamics through baroclinic pressure gradients. As in the Neelin–Held view, there is an effective moist stability and work done against this must be balanced by surface fluxes. Here, the two are inseparable and both must be included for a consistent picture. For the simplest Gill-like case, the present model is mathematically similar to these models, or even to the convergence feedback models (Webster 1981; Zebiak 1986), but it allows the parameters of these models to be defined in terms of fundamental variables. For instance, the value of the ''convergence-feedback parameter'' can be obtained from the gross moist stability, which in turn can be estimated from data. Physical interpretation is easier because the relation to the primitive equations and the parameterized effects of moist convection are clearer.

Some caveats apply to the results presented here. First, they apply only in regions where the vertical profile of temperature is constrained by convection, that is, regions where deep convective events occur sufficiently frequently in space or time that the large-scale temperature is approximately set by the deep convection. Here we use leading-order approximations under the assumption that the timescale of convective adjustment is fast compared to other processes. We know from YN and Emanuel (1993) that departures from this assumption—allowing for the effects of adjustment time—can stabilize smaller scales. Such departures from strict QE may also be important for comparing model predictions to observations (R. Brown and C.S. Bretherton 1996, personal communication). In our usage here, the timescale at which deep convection adjusts the troposphere toward the boundary layer is assumed smaller than the timescale at which surface fluxes adjust the boundary layer, to the surface conditions (on the order of a day). If these timescales are comparable (as in Raymond

1995; Emanuel 1995), then our approach remains valid if both are short compared to other timescales. Treatment of the effects of finite adjustment time in both processes will be of interest in future work.

Second, while the derivation works cleanly for the nearly inviscid time-dependent case, for the steady-state case where momentum damping is important we have used an admittedly oversimplified Rayleigh friction. This is because inclusion of a vertical viscosity representation of turbulent vertical momentum mixing significantly complicates the solutions. Numerical tests (Yu 1993) suggested that the inclusion of even a quite simple treatment of vertical viscosity can considerably improve the meridional flow relative to the simple case used here, while thermodynamic aspects and vertical structures above the PBL remain much the same as in the present solutions. Ekman pumping due to boundary layer effects does produce modifications to the solution (Yu 1993; Wang and Li 1993, 1994). The results presented here make large-scale flow in convective regions seem simple. While recognizing caveats, they offer a useful perspective on the behavior of tropical circulations.

Acknowledgments. This work was supported jointly by NSF Grant ATM-9521389 and NOAA Grant NA46GP0244. The first author (JYY) also wishes to thank the National Sciences Council in Taiwan for providing needed support toward the completion of this paper under Grants NSC85-2111-M-034-002 and NSC85-2111-M-034-003.

REFERENCES

Betts, A. K., 1986: A new convective adjustment scheme. Part I: Observational and theoretical basis. *Quart. J. Roy. Meteor. Soc.,* **112,** 677–691.

——, and M. J. Miller, 1986: A new convective adjustment scheme. Part II: Single column tests using GATE wave, BOMEX, ATEX and arctic air-mass data sets. *Quart. J. Roy. Meteor. Soc.,* **112,** 693–709.

Emanuel, K. A., 1995: The behavior of a simple hurricane model using a convective scheme based on subcloud-layer entropy equilibrium. *J. Atmos. Sci.,* **52,** 3960–3968.

——, J. D. Neelin, and C. S. Bretherton, 1994: On large-scale circulations in convecting atmospheres. *Quart. J. Roy. Meteor. Soc.,* **120,** 1111–1143.

Gill, A. E., 1980: Some simple solutions for heat-induced tropical circulation. *Quart. J. Roy. Meteor. Soc.,* **106,** 447–462.

——, and E. M. Rasmusson, 1983: The 82–83 climate anomaly in the equatorial Pacific. *Nature,* **306,** 229–234.

Jordan, C. L., 1958: Mean sounding for the West Indies area. *J. Meteor.,* **15,** 91–97.

Kleeman, R., 1991: A simple model of the atmospheric response to ENSO sea surface temperature anomalies. *J. Atmos. Sci.,* **48,** 3–18.

Lindzen, R. S., and S. Nigam, 1987: On the role of sea surface temperature gradients in forcing low-level winds and convergence in the Tropics. *J. Atmos. Sci.,* **44,** 2418–2436.

Neelin, J. D., 1989: On the interpretation of the Gill model. *J. Atmos. Sci.,* **46,** 2466–2468.

——, and I. M. Held, 1987: Modeling tropical convergence based on the moist static energy budget. *Mon. Wea. Rev.,* **115,** 3–12.

——, and J.-Y. Yu, 1994: Modes of tropical variability under convective adjustment and the Madden–Julian oscillation. Part I: Analytical theory. *J. Atmos. Sci.,* **51,** 1876–1894.

Raymond, D. J., 1994: Convective processes and tropical atmospheric circulations. *Quart. J. Roy. Meteor. Soc.,* **120,** 1431–1455.

——, 1995: Regulation of moist convection over the west Pacific warm pool. *J. Atmos. Sci.,* **52,** 3945–3959.

Wang, B., and T. Li, 1993: A simple tropical atmosphere model of relevance to short-term climate variations. *J. Atmos. Sci.,* **50,** 260–284.

——, and ——, 1994: Convective interaction with boundary-layer dynamics in the development of a tropical intraseasonal system. *J. Atmos. Sci.,* **51,** 1386–1400.

Weare, B. C., 1986: A simple model of the tropical atmosphere with circulation dependent heating and specific humidity. *J. Atmos. Sci.,* **43,** 2001–2016.

Webster, P. J., 1981: Mechanisms determining the atmospheric response to sea surface temperature anomalies. *J. Atmos. Sci.,* **38,** 554–571.

Yano, J.-I., and K. Emanuel, 1991: An improved model of the equatorial troposphere and its coupling with the stratosphere. *J. Atmos. Sci.,* **48,** 377–389.

Yu, J.-Y., 1993: The tropical atmosphere under convective adjustment. Ph.D. dissertation, University of California, Los Angeles, 205 pp.

——, and J. D. Neelin, 1994: Modes of tropical variability under convective adjustment and the Madden–Julian oscillation. Part II: Numerical results. *J. Atmos. Sci.,* **51,** 1895–1914.

Zebiak, S. E., 1982: A simple atmospheric model of relevance to El Niño. *J. Atmos. Sci.,* **39,** 2017–2027.

——, 1986: Atmospheric convergence feedback in a simple model for El Niño. *Mon. Wea. Rev.,* **114,** 1263–1271.